This article was downloaded by:
On: *21 January 2011*
Access details: *Access Details: Free Access*
Publisher *Taylor & Francis*
Informa Ltd Registered in England and Wales Registered Number: 1072954 Registered office: Mortimer House, 37-41 Mortimer Street, London W1T 3JH, UK

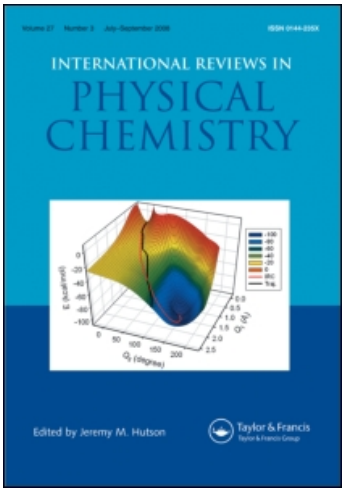

International Reviews in Physical Chemistry
Publication details, including instructions for authors and subscription information:
http://www.informaworld.com/smpp/title~content=t713724383

Detector arrays in spectroscopy

K. Birkinshaw[a]
[a] Department of Physics, University of Wales Aberystwyth, Aberystwyth, Dyfed, UK

To cite this Article Birkinshaw, K.(1996) 'Detector arrays in spectroscopy', International Reviews in Physical Chemistry, 15: 1, 13 — 40
To link to this Article: DOI: 10.1080/01442359609353172
URL: http://dx.doi.org/10.1080/01442359609353172

PLEASE SCROLL DOWN FOR ARTICLE

Full terms and conditions of use: http://www.informaworld.com/terms-and-conditions-of-access.pdf

This article may be used for research, teaching and private study purposes. Any substantial or systematic reproduction, re-distribution, re-selling, loan or sub-licensing, systematic supply or distribution in any form to anyone is expressly forbidden.

The publisher does not give any warranty express or implied or make any representation that the contents will be complete or accurate or up to date. The accuracy of any instructions, formulae and drug doses should be independently verified with primary sources. The publisher shall not be liable for any loss, actions, claims, proceedings, demand or costs or damages whatsoever or howsoever caused arising directly or indirectly in connection with or arising out of the use of this material.

INTERNATIONAL REVIEWS IN PHYSICAL CHEMISTRY, 1996, VOL. 15, NO. 1, 13–40

Detector arrays in spectroscopy

by K. BIRKINSHAW
Department of Physics, University of Wales Aberystwyth, Aberystwyth, Dyfed, SY23 3BZ, UK

Spatially dispersed spectra of ions, electrons or photons are traditionally measured by scanning the spectra across a narrow slit behind which is a detector. However, the efficiency increase offered by arrays of detectors is so large that their development is increasingly demanding the attention of spectrometer manufacturers. One-dimensional arrays of independent detectors (discrete electrode arrays) offer the highest data accumulation rate as detection can occur simultaneously at many sites, but a high resolution array of this type requires much associated electronics and this has limited the size and the market of such devices. The design and performance issues relating to discrete electrode arrays are discussed and a new high resolution array with all electronics integrated on a single silicon chip developed at Aberystwyth is described. A familiarity with silicon technology is not required by the reader. It is shown that integration brings not only advantages of scale but also of performance.

Downloaded At: 17:09 21 January 2011

1. Introduction

Spectrometers of many types are widely used in Chemistry, Physics and other disciplines for sample analysis, ionic collision research, environmental monitoring, the study of molecular structure, identification of species in distant stars etc. Most scientists will be aware of spectroscopy as a valuable research tool and in its broadest sense spectroscopy includes not only the measurement of photon wavelength but also the mass of ions, the energy of electrons etc. Photons of wavelength < 200 nm, ions, electrons etc. are here referred to collectively as particles.

Figure 1 presents an example of a *mass* spectrometer in which ions are dispersed spatially. Traditionally spatially dispersed spectra are measured by scanning the spectrum across a slit (figure 1(*a*)) behind which is typically an electron multiplier and a means of detecting the multiplier output. Ions from the source are collimated into a monoenergetic beam and dispersed by the magnet according to their momentum (and hence mass, since the initial beam is monoenergetic). A single slit detector gives an excellent resolving power which can be simply increased by reducing the slit width. However, it follows that the higher the resolving power the lower the 'collection efficiency', i.e. a smaller fraction of the spectrum passes through the slit at any given time, most being lost on the walls. This necessitates longer data acquisition times and larger samples for analysis.

An obvious but technically demanding solution to this problem is to use an array of detectors which collects a greater fraction of the dispersed spectrum as shown in figure 1(*b*).

By replacing the single slit detector with an array of detectors a much larger fraction of the spectrum can be measured. The example of figure 1(*b*) shows a 'discrete electrode' array, i.e. an array of discrete or independent electrodes. A particle falling on the microchannel plate electron multiplier (MCP) initiates a pulse of electrons from a small area of the MCP exit which falls on the electrodes and is detected. Since the early 1970s the development of such detectors has been enabled by the advent of the

0144–235X/96 $12·00 © 1996 Taylor & Francis Ltd

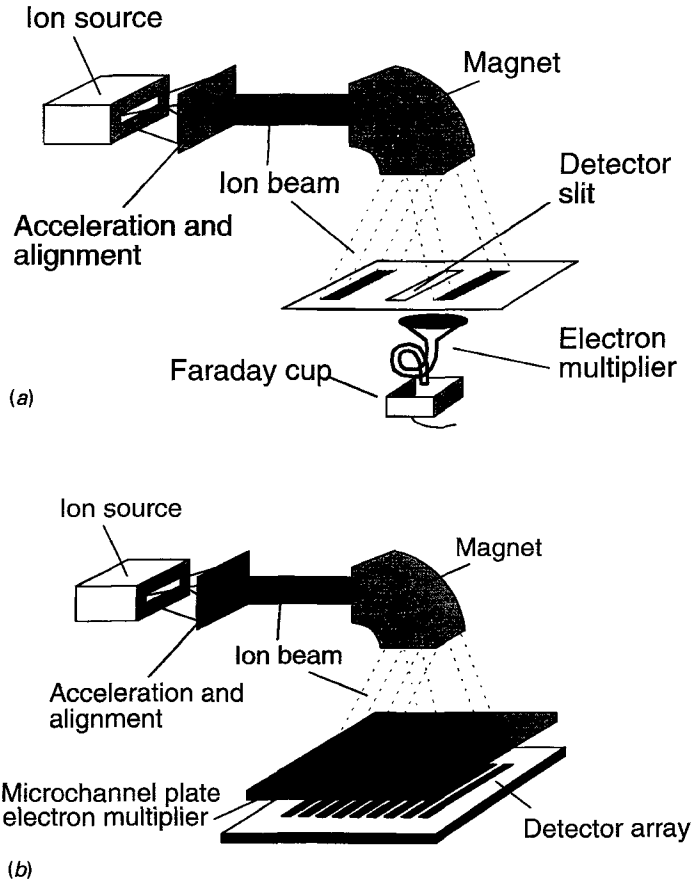

Figure 1. Simplified schematic of a magnetic sector mass spectrometer incorporating (*a*) a single slit detector, (*b*) a discrete electrode detector array. The slit of the single detector is replaced by a one-dimensional array of metal strips (electrodes) each of which has approximately the same dimensions as the single slit. Each electrode collects charge from the MCP output and forms the input to a detector circuit.

MCP and the development has been driven by the need for high efficiency detectors in UV spectroscopy [1], X-ray spectroscopy [2, 3], electron energy spectroscopy [4–6], mass spectrometry [7–11]. The need has been felt particularly in space borne experiments. The MCP (described below) enables amplification of the incoming particle flux while retaining the spatial information and is the front end of most detector arrays used for ion, electron, UV and X-ray detection.

A single slit detector has several attractive features compared with an array but has a greatly inferior collection efficiency. The attractive features are inherent and self-evident but need to be pointed out in a comparison between a single slit and an array.

- The resolving power of a single slit spectrometer is a function of the detector slit width but not a function of the electron multiplier or the detection circuitry under normal operating conditions. The resolving power of an array is a function of several experimental variables.

Downloaded At: 17:09 21 January 2011

- Each part of an array is spanned by a different part of the MCP and hence variations in quality of the MCP (gain, hot spots, faulty channels etc.) may influence the measured spectrum. In the case of a single detector all parts of the spectrum impinge on the same multiplier.
- Small variations of performance of detectors across an array can introduce structure into a spectrum. A single detector has a unique performance.

The high precision measurement of the position of an event by an array has been achieved in a number of innovative ways outlined below. Lithographic techniques used in the fabrication of integrated circuits were adapted to the fabrication of arrays of detector electrodes with a high spatial resolution (25 microns) more than twenty years ago [2] but this type of array has not been widely used due to the unmanageable amounts of associated electronics needed for a high resolution device. The integration on a single silicon chip of a complete high resolution measurement system to give an electronically and physically robust array with high performance and functionality removes this obstacle.

To manufacturers of many types of electronic instrument silicon technology has brought reductions of size, complexity, power consumption, cost etc. along with increased functionality and reliability. Enormous worldwide investment in silicon technology is enabling the development of advanced devices including micromachines, chemical and physical sensors, sensors for medicine etc. In this paper the application of silicon technology in the measurement of spatially dispersed spectra is addressed.

Charge coupled devices (CCDs) are well-known as optical image detectors in video cameras and are the most widely used optical sensor at all major astronomical observatories [12]. Technological and theoretical advances have led to large CCDs ($> 5\ cm^2$) with high light gathering efficiency, high quantum efficiency (conversion of photons to electrons) and high dynamic range. X-ray image detection [13] and ion/electron detection [14] have been achieved using CCDs. In the light of the wide availability and excellent properties of CCDs why should other types of array be under development? What advantages can they offer?

- CCDs normally operate in the wavelength range 400–1100 nm and the detection of ions and electrons by CCDs must be preceded by conversion to photons using for example a microchannel plate electron multiplier (MCP) followed by a phosphor screen. During this conversion isotropic emission of photons gives a loss of resolution.
- CCDs integrate the free electrons generated at photosites by photons. Thermal generation of electrons introduces noise into the measured signal although this can be reduced to very low levels (around 10 electrons per hour at -150 K). However, the need to cool the device is inconvenient in many applications.
- CCDs integrate charge released by the photons and they are not ideally suited to particle counting applications although they can be used in a counting mode.

One-dimensional arrays of ion counters on the other hand offer the advantage of fully parallel data acquisition with counting statistics at every detector. This paper will describe and compare existing arrays with emphasis on high resolution one-dimensional discrete electrode arrays. A new array on a silicon chip designed at Aberystwyth will be described, and design and performance issues relating to discrete electrode arrays will be outlined. It will be seen that advantages of scale, performance

Downloaded At: 17:09 21 January 2011

and cost can be realized no less in detector design than in other areas more commonly associated with silicon technology. However, this is not a paper on silicon technology. Only very straightforward issues of the layer structure of silicon chips are mentioned.

The following terms are defined in advance to maintain clarity and precision:

Array—In applications discussed below an array is preceded by a microchannel plate electron multiplier (MCP). The term 'array' is used for the device following the MCP.
Array module—The term 'array module' refers to the combination of the array plus the MCP mounted above it.
Position sensitive detector (PSD)—This is a more appropriate description of some of the devices described below which do not consist of an array of identical detectors. For convenience the generic name 'array' will be used.
Channel—The word channel is used to refer to a single MCP channel. To avoid confusion this is not used to refer to individual detectors of the array where the word 'detector' will be used.
Discrimination level or Pulse height discrimination level (PHDL)—A voltage pulse on a detector electrode above the discrimination level will be counted. A pulse below this level will not be counted.
Detection efficiency (DE)—The fraction of input events which initiate an output. For a MCP the DE_{MCP} is the fraction of particles initiating an output electron pulse. For an array the DE_{ARR} is the fraction of electron pulses initiating a detector count.
Collection efficiency (CE)—The area of the detection sites multiplied by the DE. This is a measure of the fraction of a spatially dispersed spectrum which can be simultaneously detected.
Spatial resolution—The pitch of the detector electrodes on the discrete electrode array.
Resolution—A measure of the ability of a spectrometer as a whole to resolve dispersed particles.
Resolving power—This term is used when referring to a detector in isolation from the rest of the spectrometer. Assuming a narrow particle beam the resolving power is defined here as the FWHM of the measured peak (in units of detector electrode pitch for discrete electrode arrays discussed below).
Detector electrodes/anodes—The metallic strips of a discrete electrode array used to collect the MCP electron pulses are called detector electrodes or anodes.

Downloaded At: 17:09 21 January 2011

2. Types of array

In the following the generic term 'array' is used for convenience. The term 'position sensitive detector' or PSD is more appropriate for devices which do not consist of many repeats of an identical detector and is used when referring specifically to such devices.

2.1. *1D and 2D arrays*

In most high resolution instruments where ions, electrons or photons are dispersed to obtain the distribution of mass velocity, frequency etc. the dispersion occurs only in one dimension. Two-dimensional arrays are well-known in imaging applications but are not usually 2D arrays of *discrete particle counters*. There would be two major problems in developing a two-dimensional array of discrete particle counters with a size of say 1 cm^2 and a spatial resolution of 25 microns in two dimensions namely:

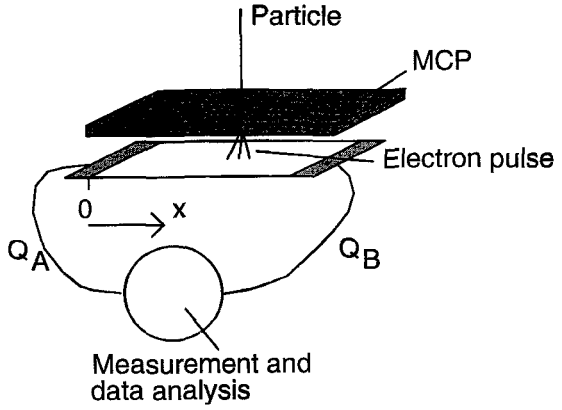

Figure 2. The resistive strip position sensitive detector.

- there is insufficient silicon area for the necessary circuitry using present technology.
- except at very low particle intensities the amount of data to shift and process would be unmanageable. If the intensity were so low that within the time taken to read the whole array there was very little chance that the same site would receive two particles then a 2D array with one counter bit per site may be conceivable.

Two-dimensional arrays are used mainly in imaging applications and present different design problems than one-dimensional arrays of particle counters. They will not be considered further except as applied to the measurement of spectra dispersed in one dimension.

2.2. *Single event 1D arrays*

These types of array have the common feature that a relatively small amount of associated electronics is required. The price paid is that the particle flux must be sufficiently low to enable the detection of a single MCP electron pulse and computation of its position of arrival before the arrival of a subsequent pulse. The accuracy of the computed position is improved for higher gain pulses and generally is not degraded by spreading of the electron pulse. Single event arrays have a high collection efficiency and a high resolving power at a low cost but have a maximum count rate for the whole array of only about 10^5 cps.

2.2.1. *Resistive strip*

In its simplest form (figure 2) this consists of a thin layer of resistive material on the surface of an insulator with electrodes attached to each end [15]. The path resistance to each end of the strip depends on the position of arrival of a pulse of electrons and this position can be computed simply from the magnitudes of the charges arriving at each end. A 'spatial location error' of about 21 microns over 25 mm has been obtained with this device [16].

The speed is limited by the RC time of the resistive strip. Thermal fluctuations in the resistive strip are the primary source of noise. Distortions of the image introduced by a rectangular resistive strip can be compensated by using resistive strips of different shape [17].

Downloaded At: 17:09 21 January 2011

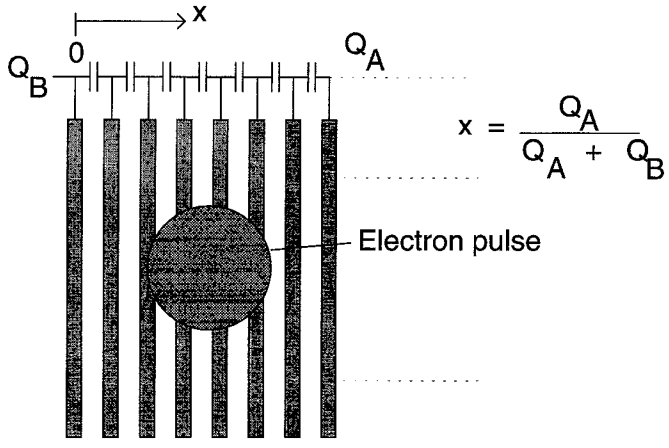

Figure 3. Schematic of a capacitatively coupled discrete anode array.

Commercially available photosensitive position sensitive detectors with a p-type semiconductor resistive material claim a 'position resolution' (minimum detectable displacement) of about 7 microns and a 'maximum position detection' error of 500 microns for a position sensitive detector of dimension 2·5 × 34 mm [18].

Downloaded At: 17:09 21 January 2011

2.2.2. *Discrete anodes*

Electron charge from the MCP is collected on a set of electrodes which may be wires or metal strips (figure 3) on an appropriate medium [19]. These strips may be interconnected by capacitors which allow very rapid transfer of signal to amplifiers at each end. The position of arrival is simply calculated from the charges arriving at the amplifiers. Electrodes are metallic and resolving power is not subject to the thermal noise inherent in resistive strip PSDs. The broadening of measured peaks is generally determined by the amplifier noise, typically amounting to 10^3–10^4 electrons rms. Van Hoof and Van der Wiel [20] describe a PSD with anodes set in a radial arrangement for use in angle resolved electron spectroscopy.

Electrodes may also be interconnected by resistors to give a device similar to the resistive strip PSD but without geometrical distortion.

2.2.3. *Coincidence arrays—multi-anode microchannel plate array (MAMA)*

The position of an event in two dimensions has been found [3, 19] using a grid of crossed wires. With a grid of $n \times m$ wires the positions of arrival at $n \times m$ points can be found using $n+m$ amplifiers. Coincident signals on the orthogonal wires indicate real events. A resolving power of 10 microns has been achieved [3] using a crossed grid of 100 micron wires on a 200 micron pitch. Logic was provided to decode the event position and the device could count at rates up to 10^4 s^{-1}.

Timothy and Bybee [21] have described a family of 'multi-anode microchannel arrays' (MAMAs) for one- and two-dimensional imaging. The location of an event is determined by the simultaneous detection of a charge pulse on two sets of anodes deposited on a ceramic substrate. The spatial resolution of the anodes was 25 microns. Anode configurations are described which enable one-dimensional detection at $n \times m$ locations using $n+m$ electrodes as shown in figure 4 for a sixteen anode device. Electrodes were connected alternately to coarse and fine position encoding amplifiers as shown. The ambiguity in the location of an event when measured by the fine

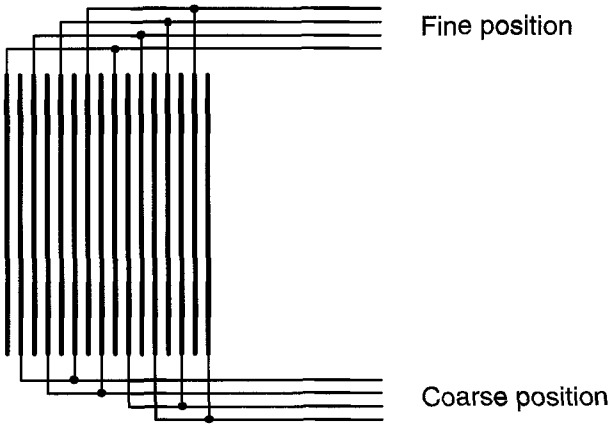

Figure 4. Schematic of a coincidence anode array.

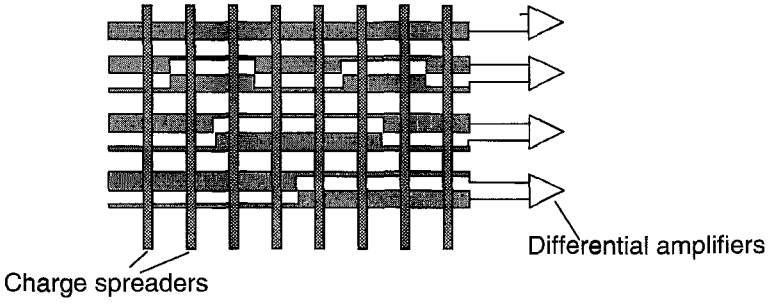

Figure 5. The coded anode array. Charge spreaders are electrically insulated from but capacitatively coupled to underlying coded metal strips

Downloaded At: 17:09 21 January 2011

position encoder was resolved by the coarse position encoder. The final ambiguity of whether the event is closer to the fine position electrode or the coarse position electrode was resolved by determining the electrode receiving the greater charge.

Two-dimensional detection was achieved by using a multi-layer electrode arrangement as follows:

(*a*) An additional set of discrete electrodes was fabricated perpendicular to the electrodes shown in figure 4. The additional electrodes were separated from coincidence anode array by an insulator but exposed at the interstices to collect electrons.

(*b*) Two coincidence arrays of the type shown in figure 4 were laid out orthogonally separated by a layer of insulator.

2.2.4. *Coded anodes—(CODACON)*

A further method of calculating the position of arrival of an electron pulse is to shape the detector electrodes in such a way that the position of arrival is given by division of charge between them and is output as a binary code [1]. This has been achieved to an accuracy of 25 microns in one dimension as shown in figure 5. Electron pulses from the MCP fall on charge spreaders which are capacitatively coupled to the underlying coded metal strips arranged in pairs. The induced signal on each track of a given pair differs due to the different overlap with the charge spreaders. Each

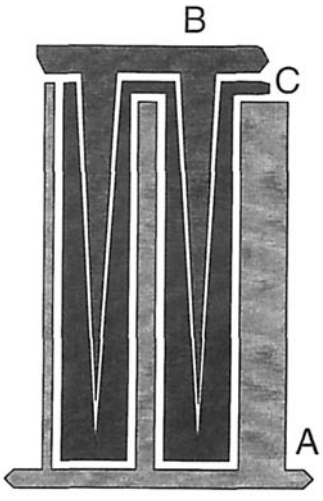

Figure 6. A three electrode wedge and strip array (not to scale).

Downloaded At: 17:09 21 January 2011

differential amplifier picks up this difference and the bit pattern output by the comparators identifies the position of the electron pulse. The device used by McLintock *et al.* contained 1024 charge spreaders on a pitch of 25·4 microns and 10 pairs of underlying coded anodes.

2.2.5. *Wedge and strip*

A resolving power of about 20–50 microns in *two* dimensions has been achieved using the 'wedge and strip' device of figure 6 [22]. Devices of size up to 35 mm square have been described. An electron pulse falling on the device divides its charge between electrodes A, B and C allowing computation of the position of the pulse by the signal processing electronics. The electron pulse must be sufficiently wide to span several wedges and strips or a periodicity is introduced into the position measurement. A number of electrode configurations are described with appropriate expressions for the position of arrival of the electron pulse. Electrodes are metallic and signals are not subject to the thermal noise inherent in resistive strip PSDs. There is also no dependence on the uniformity of the metallic electrodes as there is on that of a resistive strip. The main contribution to random position errors is the amplifier noise. Martin *et al.* [22] obtained position errors which varied with MCP gain from about 200 microns for a gain of 10^6 to about 30 microns for a grain of 5×10^6.

2.3. *Multiple event 1D arrays*

This type of array is characterized by an extremely high count rate capability. It is not restricted to detect one event at a time for the whole array but can detect events simultaneously at every detector site.

In the case of a high resolution multiple event array each detector site is spanned by a small area of MCP. For example a detector electrode of dimension 2 mm × 25 microns would typically be served by < 1000 MCP channels. As shown below each MCP channel requires typically 0·01 s recovery time between events and hence the maximum count rate at each detector is limited to about 10^5 Hz by the MCP—twenty times lower than the maximum rate of a single Aberystwyth detector. A single event

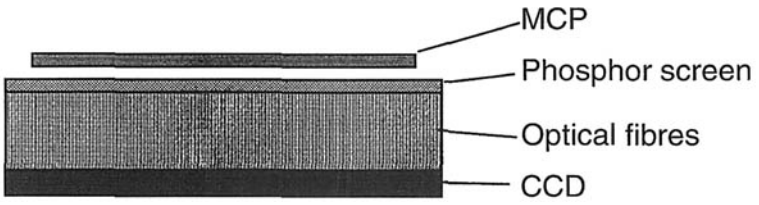

Figure 7. An electro-optical detector array.

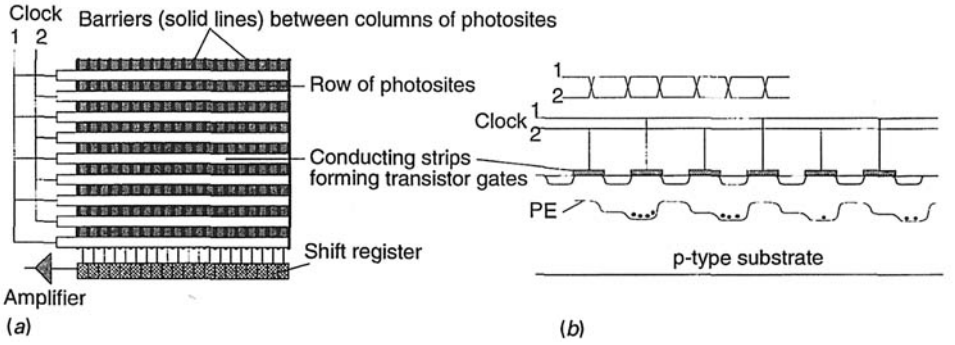

Figure 8. (*a*) Schematic of a CCD. (*b*) Free electrons are trapped in potential wells. The wells are moved along a column of photosites by the application of clock pulses to the transistor gates thereby transporting free electrons to the shift register.

array is serviced by the MCP channels above its entire area—of the order of 10^6 channels—and the detection and position computation time determines the upper count rate limit of the module.

2.3.1. *Electro-optical*

In this device (figure 7) the MCP output pulses are accelerated onto a phosphor screen and the resulting pulse of photons is channelled down an optical fibre bundle to a photodiode array or a CCD [11, 23]. Resolution is lost at each interface and the photon pulse width measured is a minimum of 100 microns. This resolution combined with a good dynamic range has enabled the use of these devices in mass spectrometers. A useful characteristic of this type of array is that in applications where bunches of ions arrive at the detector in a very short time (e.g. 2 ns) the total charge of the electron pulses would be correctly integrated whereas the discrete anode multiple event array (below) would register only one event.

Typically a CCD (figure 8) may contain 400 columns each with 400 photosites with each photosite of dimension 25 microns × 25 microns. Barriers between the columns isolate the columns from each other and horizontal conducting strips (which separate the rows of photosites) form the gates of field effect transistors. The direction of dispersion in figure 8(*a*) is horizontal. Light falling on the photosites is converted into electron–hole pairs and the free electrons are trapped in potential wells created by the transistor gates. By applying pulses to the transistor gates as shown in figure 8(*b*) the potential well carrying the free electrons is moved towards the shift register. On each clock cycle new packets of charge are dumped from the columns onto the shift register which is rapidly shifted through the amplifier where it may be output as an analogue or digital signal. For each step along a column 99·998 % of electrons successfully move to the next potential well giving an error of about 1 % for 400 shifts.

Downloaded At: 17:09 21 January 2011

Thermal generation of electrons at −20 °C is typically about 30 electrons per photosite per second and this approximately doubles for each 8° rise in temperature. The capacity of a photosite is typically about 300000 electrons (for a 25 micron × 25 micron well). Above this limit the electrons migrate to adjacent channels causing a 'blooming' effect. Readout noise generated in the amplifier is typically about 80 electrons rms.

The CCD can be operated in two modes. At low particle intensity the MCP can be operated at high gain and the accelerating voltage between the MCP and the phosphor screen can be maintained high giving large photon pulses which can be counted. At higher particle intensities the MCP gain and the electron accelerating voltage can be reduced giving a lower photon pulse intensity. Charge can then be integrated with the total free electrons being a measure of the particle flux.

2.3.2. *Discrete anodes*

Discrete anode multiple event arrays consist of many single metal strips (e.g. wires or strips laid out on an insulating substrate) laid side by side to collect the MCP output [2, 4, 7, 10, 24, 25]. Each metal strip has its own data logging circuitry. In concept this is analogous to the traditional single slit detector repeated with as high a spatial resolution as technology allows. Small, low resolution arrays of this type present relatively little problem of design or fabrication. However, the design of larger high resolution devices is much more demanding. Timothy and Bybee [20] have produced 1D and 2D devices. The 2D discrete anode array consists of a 10 × 10 array of metal anodes, each anode being of dimension 1·2 mm × 1·2 mm [20]. This is preceded by a curved channel MCP. Each anode has its own external charge amplifier, discriminator and data logging system. These devices have a maximum count rate at each detector site of $1{\cdot}4 \times 10^6$ cps. 1D discrete anode arrays containing 160 electrodes of dimension 8 mm × 0·1 mm were also produced, each anode having its own external amplifier and data logger. The length of non-integrated discrete electrode arrays is limited by the amount of external electronics required.

Hatfield *et al.* have produced an array of 32 detectors with spatial resolution 160 microns on a silicon chip and have used it in the study of electron energy loss spectra [26]. Charge pulse sensors consist of a preamplifier stage and a comparator stage and the output of each sensor is routed to an 8 bit counter. The device requires set-up, data acquisition and read cycles and there is no protection against counter overflow.

2.3.3. *The Aberystwyth array*

A 5 mm integrated array of 192 detectors on a single silicon chip has been successfully produced at Aberystwyth and is fully integrated including detector electrodes and all sensing, counting, bus interface and control circuitry on a silicon chip. It is a small, low power, high resolution array which realizes the advantages of a fully parallel system and is described below. Each detector is independent and consists of a metal strip (detector electrode) exposed to the MCP output, a charge sensor, an 8 bit counter, control logic and a bus interface. The detector electrode pitch is 25 microns. It is shown below that the diameters of electron pulses arriving at the array electrodes are typically several electrodes wide and hence a single event may generate a single count at several detectors. The main source of noise is MCP dark counts.

Downloaded At: 17:09 21 January 2011

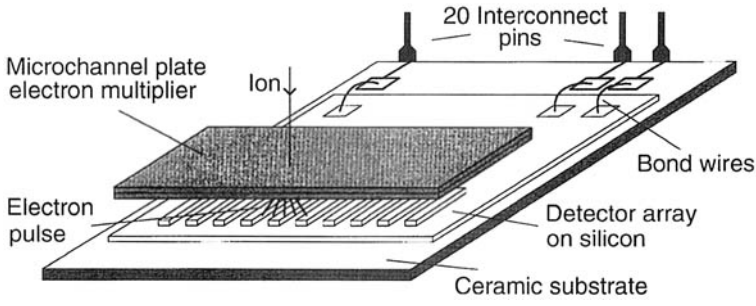

Figure 9. A schematic of the Aberystwyth discrete electrode detector array. To provide mechanical robustness the fragile bond wires are encapsulated in a bakeable epoxy.

3. Performance

The performance of arrays cannot be characterized as straightforwardly as a single detector. Factors influencing performance parameters are outlined in this section.

3.1. *Collection efficiency (CE) and detection efficiency (DE)*

A detector array can measure a much greater fraction of a spectrum than a single slit and is said to have a greater collection efficiency. Improvement of collection efficiency (CE) has been the driving force behind the development of detector arrays. The primary objective has been to develop *larger* arrays in order to detect a larger fraction of the spectrum simultaneously. However, the size is only one parameter influencing the collection efficiency. The detection efficiencies of both the MCP and the array must be considered. In the following it is assumed that the MCP completely covers the detection sites of the array.

3.1.1. *The MCP*

The detection efficiency (DE_{MCP}) of the MCP is defined here as the fraction of impacting particles which initiate an output electron pulse. The open area ratio (OAR) is the ratio of the open MCP channel area to the total plate area and is typically around 70%. Particles not entering a MCP channel but instead striking the interstitial material are detected with lower, but not zero, efficiency [27] as they also may release secondary electrons. Detection efficiency varies with the type of particle detected, the energy of the particle, the angle of impact with the MCP channel wall and the channel wall coating [2, 28, 29]. Typically ions and electrons may be detected with a higher efficiency than UV and X-rays and optimum angles of incidence are of the order of 10°.

3.1.2. *The array*

The collection efficiency of the array (CE_{arr}) is defined here as:

$$CE_{arr} = A_{arr} \times DE_{arr}$$

where

CE_{arr} = collection efficiency of the array;
A_{arr} = the array area; and
DE_{arr} = detection efficiency of the array.

The detection efficiency of the array (DE_{arr}) is defined here as the fraction of the MCP

Downloaded At: 17:09 21 January 2011

output electron pulses which initiate a count in one or more detectors. DE_{arr} depends on a number of factors, for example the gain of the MCP, the detector discrimination level, the particle flux, the dead time (e.g. time lost during reading of the array) etc.

A single event logging array can log only one event at a time arriving at the array. Such arrays can have a high detection efficiency but only at a low particle flux. Each detector of a discrete electrode array can log counts at a higher rate than the whole of a single event array.

3.1.3. *The array module*

The collection efficiency of the array module is defined here as the fraction of particles falling on the front face of the MCP (within the area directly above the detector sites) which initiate a count on one or more detectors and is given by:

$$CE_{mod} = A_{arr} \times DE_{arr} \times DE_{MCP} = CE_{arr} \times DE_{MCP}$$

where CE_{mod} = collection efficiency of the array module (array + MCP).

3.2. *Dynamic range*

The dynamic range of a detector is the range over which a signal can be accurately measured and is defined as the ratio of the maximum signal detectable in the linear region to that at which the signal-to-noise ratio is 1. Clearly the random nature of the particle arrival times will influence the dynamic range but this is not considered here as the conclusions reached are not affected significantly. A high dynamic range is essential in quantitative spectrometry in order to correctly measure the relative heights of weak and intense peaks. The dynamic range of the *system* again depends on the components which include:

- the MCP
- the array
- the data acquisition system

The maximum count rate of the system is limited by the slowest component. For a small multiple event discrete electrode array module the MCP response limits this. For larger discrete electrode arrays the data readout rate becomes the limiting factor as data must be read from all counters before any are filled. For single event arrays/position sensitive detectors, it is the data acquisition and position computation time which limits the maximum count rate. In an electro-optical array (§2.3.1) the CCD imposes no upper limit on the rate of arrival of particles at the MCP input (the free electron storage capacity of a photosite must not be exceeded). Many photons arriving at CCD photosites simultaneously will generate free electrons with the same quantum efficiencies as they would have if arriving singly. However, the MCP output will become nonlinear with large incident particle fluxes.

The minimum count rate as defined above is limited by the noisiest component. This is generally the MCP in the case of arrays working in the counting mode. For detectors working in the analogue mode other sources of noise dominate as described above.

3.3. *Resolution*

'Resolution' refers to the ability of spectrometers to separate particles of different mass, energy, wavelength etc. The definition of resolution is somewhat arbitrary. The resolution of a mass spectrometer is normally taken as $M/\Delta M$ where ΔM is the mass separation of two peaks which overlap to give a 10% valley between the peaks. The

Downloaded At: 17:09 21 January 2011

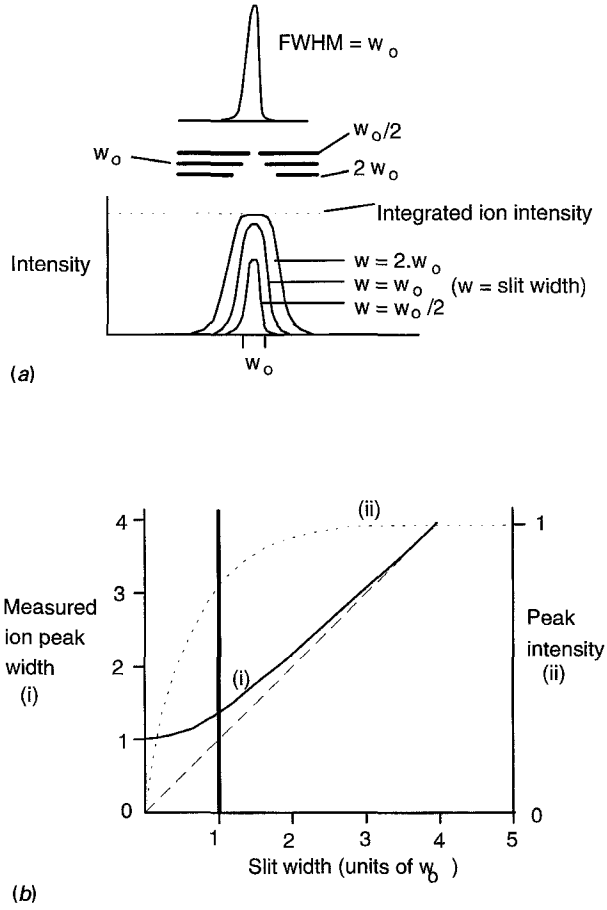

Figure 10. The influence of the detector slit width on the measured ion peak width and peak intensity. (*a*) schematic representation showing ion peaks, (*b*) graphical representation of measured ion peak width (solid curve (i)) and peak intensity (dotted curve (ii)). The vertical bar indicates that a choice of detector slit width equal to the ion beam FWHM gives a reasonable compromise between the measured peak width and peak intensity.

resolution defined for a diffraction grating and known as the Rayleigh criterion is $\lambda/\Delta\lambda$ where $\Delta\lambda$ is the difference in wavelength between two lines whose central maxima fall on the first minimum of the other line. The latter gives an 80% valley.

In the case of a single slit detector the detector parameter influencing the resolution is the slit width. The influence of detector slit width on the peak shape is shown in figure 10(*a*). As the detector slit width is increased the measured peak intensity increases at the expense of a greater peak width. At a sufficiently low slit width further reduction gives reduced peak intensity (curve (ii)) but the measured peak width remains essentially constant (curve (i)) as shown in figure 10(*b*). Increasing the detector slit width above the width of the particle beam gives an increase in peak width but no increase of peak intensity. The vertical solid line in figure 10(*b*) shows that a detector slit width equal to the particle beam FWHM gives a reasonable compromise between the measured peak width and peak intensity. A slit width of about 10 microns is typical of a high resolution mass spectrometer. A lower width limit of about 1 micron is set by the quality of the slit edge.

Downloaded At: 17:09 21 January 2011

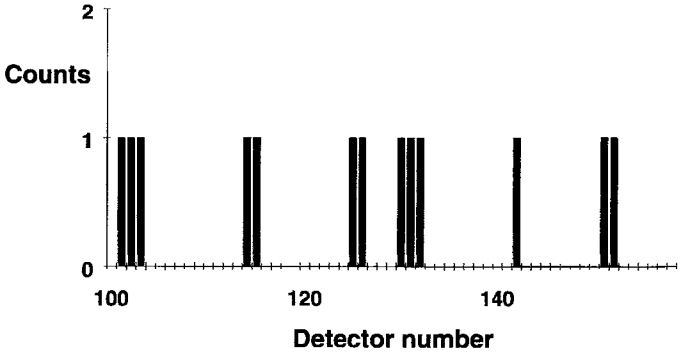

Figure 11. Single electron pulses recorded by the array. Each pulse is registered as a single count on N ($N = 1$, 2 and 3 in this case) detectors depending on the MCP gain. Events with $N = 0$ are of course not observable.

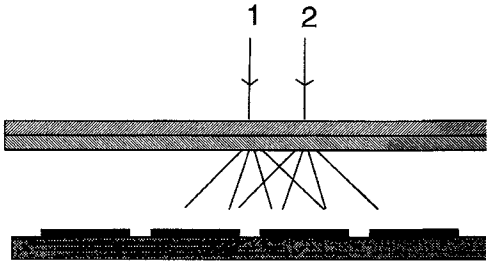

Figure 12. The locations of particles arriving at positions 1 and 2 will be computed accurately. The location of particles arriving in the region between these positions are computed at position 1 or 2.

In the case of a discrete electrode array the detector slit is absent and two modes of data acquisition result in different resolving powers:

(*a*) Observe single events, compute and record the centre of mass of the pulse group. A single electron pulse activates N detectors (i.e. generates a single count on N detectors) in the vicinity of the event where $N = 0, 1, 2, \ldots$. Figure 11 shows single events recorded at a low ion intensity. Each event is recorded as a single count on N detectors where $N = 1, 2, 3, \ldots$. Events with $N = 0$ are unobservable. With the exception of the case $N = 1$, the location of the event can be found to an accuracy of about $\pm\frac{1}{4}$ electrode width as shown in figure 12. A particle arriving at position 1 (at the midpoint between two electrodes) will activate the same number of detectors on either side of the point of arrival and hence its position would be computed accurately. Similarly the position of a particle arriving at position 2 would be computed accurately. A particle arriving between these two positions will have a computed position at position 1 or 2. This can be understood as follows. The gains of the MCP pulses are distributed about the mean with lower gain pulses activating less detectors than pulses of a higher gain. It is assumed that an electron pulse is roughly symmetrically distributed (spatially) about the centre, and therefore as the pulse widens (for larger gains) N increases by alternately incrementing at each side of the pulse group. This mode of data acquisition is currently under test and will not be discussed further here. Most work at Aberystwyth has been carried out in the event accumulation mode described in the following section.

Downloaded At: 17:09 21 January 2011

(*b*) Accumulate many events and record the resulting peak. The detectors *store* the counts generated by each event. A peak is accumulated and information on the location of each event is lost. In this mode the recorded peak is wider than in mode (a) and hence the resolving power is lower. This can be easily seen in the hypothetical case of an infinitely narrow particle beam. Mode (a) would give a measured peak approximately half a detector electrode wide while mode (b) would give a measured peak typically several detectors wide (see below). The dynamic range of the array is greater in this mode.

3.4. *Region of stable operation*

Normally the existence of a stable operating region is associated with a plateau of the measured particle intensity as a function of the operating conditions, e.g. as a function of the MCP supply voltage and detector discrimination level. If a plateau exists then for a small fluctuation of operating conditions there will be a negligible change of measured intensity. In the case of a multiple event discrete electrode array it is shown below that for a narrow particle beam plateaux are indeed expected [30] but for a wide particle beam plateaux are not expected.

Downloaded At: 17:09 21 January 2011

4. The microchannel plate electron multiplier (MCP)

Single particles cannot be measured with currently available arrays without prior amplification using an electron multiplier. The advent of the MCP in the 1960s marks the beginning of array detection as MCPs both amplify the particle signal and retain the spatial information.

The MCP is an integral part of a detector array module and its performance often dominates the performance of the module. There has been extensive coverage of the performance characteristics of MCPs [28, 31–33] and the following only outlines factors relevant to the operation of a multiple event discrete electrode array.

4.1. *Straight channel MCPs*

A schematic of a MCP is shown in figure 13(*a*). It consists of a plate typically of thickness $L = 0{\cdot}5$ mm and composed of many small tubes (typically straight tubes of diameter $D = 12$ microns) each of which is at an angle of typically 10° to the vertical and has an internal coating of a low work function material. A voltage (typically $\leqslant 1$ kV) is applied between the metallized front and rear surfaces of the MCP. A particle entering a channel and striking the inside wall may release one or more secondary electrons which will be accelerated down the tube and in turn release more electrons, ultimately leading to a shower of G (gain) electrons at the output. For a given MCP voltage the gain versus L/D passes through an extremum [28, 32]. Hence by manufacturing MCPs with L/D at the extremum value the gain is insensitive to small variations of channel characteristics which inevitably occur due to manufacturing tolerances. At a MCP voltage of around 1 kV a value of $L/D \approx 40$–60 is found to be appropriate.

In the pulsed mode a MCP channel delivers a saturated charge pulse (a gain (G) of up to about 10^5). A single MCP plate cannot reach saturation i.e. a single particle does not release sufficient secondary electrons to enable a channel to saturate. As the gain is increased by increasing the supply voltage, ions formed from residual gas are accelerated back up the channels and initiate spurious pulses. Saturation can be reached using MCP stacks as the channels of the second MCP are activated by many

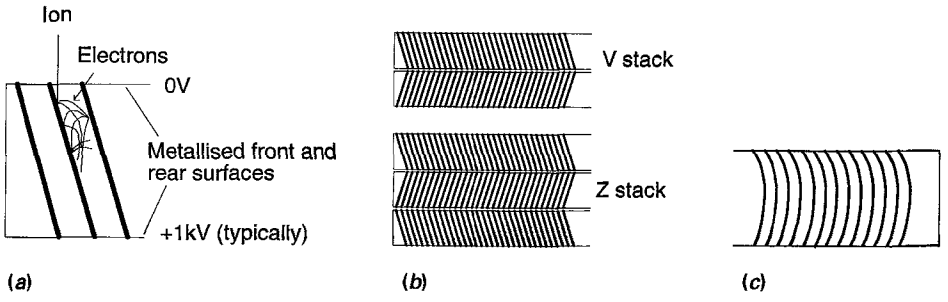

Figure 13. Microchannel array electron multipliers, (*a*) single plate straight channel MCP; (*b*) MCP stacks. The channels are set to slope in opposite directions to reduce the effect known as 'ion feedback' in which ions produced by collision of electrons with residual gas molecules are accelerated back up the channels to initiate further pulses; (*c*) curved channel MCP.

electrons from the first. However, resolution is reduced as the output of the final MCP is several MCP channels wide. It has been shown [32, 34] that the saturated gain is proportional to the channel diameter. Table 1 gives examples of performance of MCP stacks.

The magnitude of a saturated pulse is self-limiting [32, 34]. The main factors limiting the gain are:

- the negative space charge of electrons within a channel increases the electric field along the channel towards the output end but reduces it towards the input end. When the field towards the input end approaches zero no further multiplication occurs.
- the conductivity of the channel wall. This is proportional to L/D and limits the mean output current. It is the current along the channel which 'recharges' the channel. Clearly the mean output current cannot exceed the channel wall current plus the input particle current.

When channels are operated in saturation pulse height distribution is independent of the initiating events and is peaked with a 'resolution' ($\Delta G/G$) typically between 30% and 120%. After firing the channel requires time to recover (typically 0·01 s) during which the charge removed from the channel is replenished through the channel wall current in much the same way as a capacitor is recharged. This limits the maximum channel count rate beyond which the gain decreases.

Detection efficiency is dependent on the type, energy and angle of incidence of impacting particles. The optimum angle is typically between 5° and 15° and has been published for various particles over a range of energies [28, 29, 35]. A standard low work function coating allows detection of electrons and ions with efficiency between 5% and 80%. The optimum energy for electrons is 0·5–4 Kev. For positive ions the optimum energy range is 10–50 Kev [29]. Photons of wavelength 180 nm have a detection efficiency of about 0·01% with a standard coating and this falls rapidly with increasing wavelength. Special coatings of CsI increase the detection efficiency by about three orders of magnitude [35] and enable the detection of 220 nm photons with an efficiency of 0·01%. However, these coatings require careful attention and deteriorate on exposure to atmospheric moisture. The MCP performance is also influenced by other factors:

Downloaded At: 17:09 21 January 2011

Downloaded At: 17:09 21 January 2011

Table 1. Typical characteristics of MCP stacks in pulse mode operation. Characteristics vary substantially with experimental set-up. The following characteristics should be seen as a guide.

MCP type	G (approx)	ΔG (approx)	Channel diameter	L/D	Comments	Ref.
Single MCP (straight channel)	(max gain approx. 10^4)	Negative exponential	12 μ	40:1	Above a gain of 10^4 the output becomes unstable due to ion feedback effects.	[28]
Single MCP (curved channel)	1×10^6–2×10^6	34–93%	25 μ	80:1	Gain distribution is quasi-Gaussian. MCPs with $\alpha = 140$ have been produced.	[27]
2 stack	10^6–10^7	120–150%	12 μ	40:1	Gain distribution is quasi-Gaussian.	[28]
3 stack	$> 5 \times 10^7$	< 120%	5–10 μ	40:1	Gain distribution is quasi-Gaussian.	[29]
3 stack	$> 2 \times 10^8$	< 60%	5–10 μ	60:1	Gain distribution is quasi-Gaussian.	[29]
2 stack + 2 stack combination	$\sim 5 \times 10^7$	< 120%	12 μ	40:1	Gain distribution is quasi-Gaussian.	[15]
2 stack + 3 stack combination	$\sim 3 \times 10^7$	< 120%	12 μ	40:1	Gain distribution is quasi-Gaussian.	[15]

- To achieve and maintain a high performance, correct conditioning of a MCP before use is essential. The lifetime of the MCP is also extended by careful conditioning [27].
- Ions of mass > 250000 Daltons are very inefficient in releasing secondary electrons and activating an MCP channel.

4.2. *Curved channel MCPs*

Single plate MCPs with curved channels (figure 13(*c*)) have been described with $L/D = 80$–140 [27]. In these devices the gain is not limited by ion feedback to about 10^5 as ions are not accelerated far along the tube before colliding with the wall. Saturated gains of $> 10^6$ have been achieved. Although the gain is larger than single straight channel MCPs with $L/D = 40$, the dynamic range is smaller due to the higher resistance and greater recovery time of channels with $L/D = 80$–140.

5. The Aberystwyth discrete electrode array

A high performance array must have the following characteristics:

- high resolving power
- high dynamic range
- stable operating region
- uniform performance across the array
- high functionality
- low size, weight, complexity and power consumption
- easily testable
- robust mechanically and electrically.

The design of the Aberystwyth array and the performance achieved is described in this section. Work on the array has been published in a series of publications [25, 30, 36–41].

5.1. *Design*

To understand the structure and performance of a detector array on a silicon chip it is not necessary to be familiar with the process by which a silicon chip is designed and fabricated. The relevant features of the Aberystwyth array are shown as a simplified schematic diagram in figure 14.

The detector array chips are cut from a silicon wafer and the underside of the array chip (the silicon substrate) is the wafer material (typically 0·3–0·5 mm thick). Circuitry is placed at the top surface of the silicon substrate and is covered by a 4·5 micron thick insulating layer of polyimide. Aluminium (~ 1 micron thick) is deposited on this insulating layer and detector electrodes are formed by etching away unwanted metal. Contacts to the underlying circuitry are made through holes (vias) in the insulator. A second layer of polyimide (the passivation layer) is deposited on the top surface of the array. This layer (which serves to protect circuitry) is also 4·5 microns thick and sections of this layer are etched away to reveal the detector electrodes and the sites to which the bond wires are welded. Array chips are stuck onto a piece of ceramic of dimension 50 mm × 50 mm × 1 mm. Bond wires form contacts from the chip to metal tracks on the ceramic which in turn terminate in connector pins at the edge of the ceramic providing connections to the outside world.

The detector electrodes are of dimension 2 mm × 18 micron × 1 micron and are distributed along one side of the chip on a 25 micron pitch. Each electrode has its own charge pulse sensor, 8 bit counter, control logic and bus interface. An electron pulse

Downloaded At: 17:09 21 January 2011

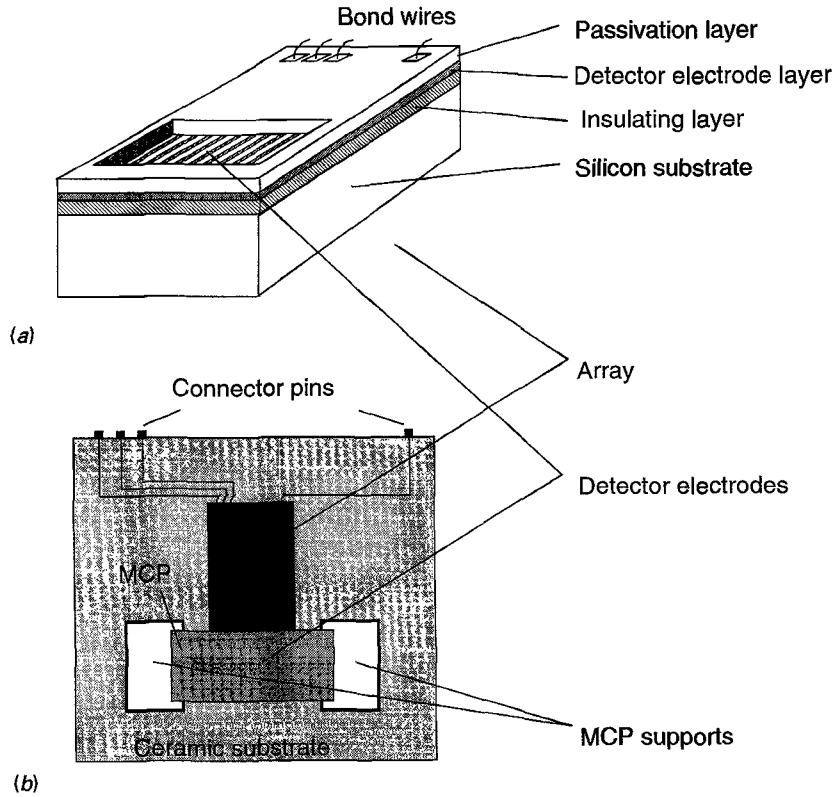

Figure 14. (*a*) Schematic representation of the silicon chip (not to scale) with detector electrodes exposed through the passivation layer. Both the passivation layer and the insulating layer are of polyimide with a thickness of 4·5 microns. The silicon substrate is about 300 microns thick. The detector electrode layer (aluminium) is about 1 micron thick. Most of this layer is etched away to leave the detector electrodes. (*b*) Schematic diagram of the MCP mounted on metal supports above the detector array.

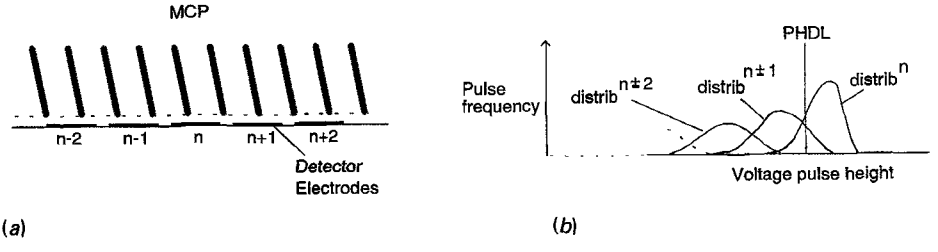

Figure 15. Schematic representation of the array module and voltage pulse height distributions on detector electrodes. Pulses above the PHDL will be registered, others will be rejected. (*a*) The exit of the second MCP (a double MCP stack was used) and the detector electrodes on the surface of the silicon chip are shown approximately to scale for the conditions given in the text. The labels n, $n \pm 1$ etc. identify the detector electrodes for the purpose of discussion. (*b*) Pulse height distributions. This figure is valid in two cases: (i) illumination by a particle beam one electrode wide and centred above electrode n; (ii) uniform illumination of the array with particles.

Downloaded At: 17:09 21 January 2011

from the MCP is collected on the electrodes and if the induced voltage on any electrode is greater than the PHDL of its associated sensor then a cycle is initiated in which the sensor transmits a 5 V output pulse to an 8 bit counter and discharges the collected electrons. Any charge insufficient to trigger a pulse is discharged to prevent charge build-up. The capacitance of a detector electrode is about 0·4 pF. To facilitate bench testing each detector electrode is capacitively coupled to an underlying metal 'finger' to allow the application of test pulses. Pulses from the charge sensors are routed to associated 8 bit counters arranged in banks. A local bus is associated with each counter bank and each local bus is buffered onto the main bus. The main bus is, in turn, buffered through an interface and I/O pads onto a bus on the ceramic substrate which can be connected directly to a PC.

Each detector of the Aberystwyth array is a self-contained ion counter. All detectors are controlled and read via a 20 bit bus. To prevent overflow, counters are designed to stop counting when 254 counts have been accumulated. Counters are read sequentially. The array can operate in three modes:

MODE 1—when the external controller recognizes that one of the counters has reached 254 counts it inhibits all further counting and then reads all the accumulated counts. This gives a mass spectrum with all peaks relatively correct.
MODE 2—the counters are read cyclically and continuously. This mode will detect low intensity ions at maximum efficiency but intense peaks may saturate.
MODE 3—Counters are enabled for a fixed period of time.

In all modes counters are automatically reset after they have been read. Most experiments have been carried out in mode 3. In the present array some noise is introduced into the spectrum by read clock pulses during data accumulation in mode 2.

The array is designed to interface directly to a computer. A single chip containing 192 detectors is of dimension 14 mm × 5 mm × 0·3 mm, of weight $\approx$ 0·05 g, and under normal operating conditions consumes $<$ 5 mW of power. The fragile bond wires shown in figures 9 and 14 are encapsulated in a bakeable epoxy to give a mechanically robust device. Electrical robustness is provided by diode protection against high voltage excursions. The array chip itself is bakeable to at least 150 °C but the upper temperature limit of the module is determined by the adhesive used to secure the chip to the ceramic substrate. No attempt has yet been made to produce a bakeable module.

5.2. *Pulse height distributions*

An electron pulse output by the MCP in general is divided between several detector electrodes and induces voltage pulses whose magnitude decreases with increasing distance from the pulse centre. Figure 15(*a*) is a schematic of the environment at the MCP output. The diagram is approximately to scale for the MCP channel diameter of 12 microns, the channel pitch of 15 microns, the MCP/array separation of 4·5 microns, the detector electrode width of 18 microns and the electrode pitch of 25 microns. An understanding of the pulse height distribution is essential to an understanding of the resolving power. A schematic of a distribution of voltage pulse heights for many events is shown in figure 15(*b*).

Figure 15(*b*) can be interpreted in two distinct ways:

(i) A particle beam about one electrode wide (for the purposes of discussion) and centred directly above electrode *n* gives the highest voltage pulses on electrode *n* and lower voltage pulses on more remote electrodes. The distribution on the

Downloaded At: 17:09 21 January 2011

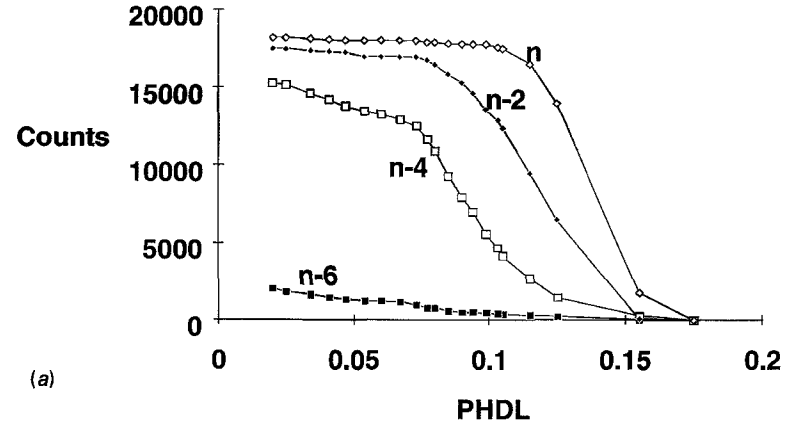

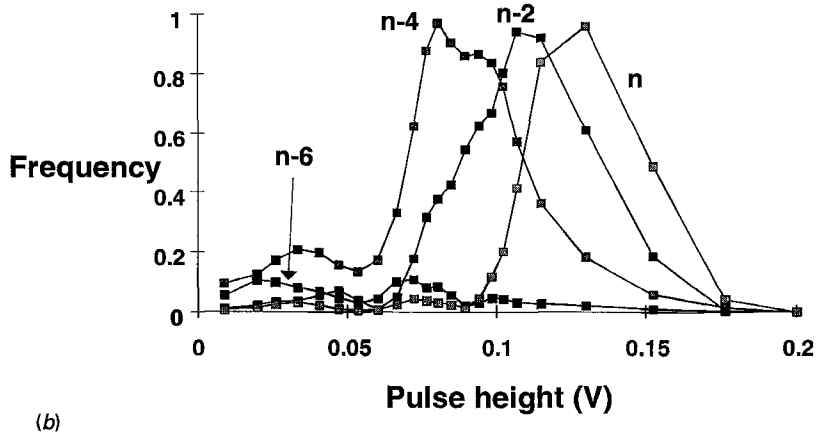

Downloaded At: 17:09 21 January 2011

Figure 16. (*a*) Observed variations of measured counts (for a fixed measurement interval) as a function of discrimination level (PHDL) for a narrow ion beam. Peak counts and counts on adjacent detectors are shown. (*b*) Pulse height distributions scale maximum normalized to unity obtained by differentiating the curves of (*a*). The MCP supply voltage is 2·4 kV and the MCP/array separation was between 25 and 50 microns.

right of figure 15(*b*) is the distribution of voltage pulse heights on electrode *n* and the other distributions refer to the electrodes indicated.

(ii) Uniform illumination of the array gives a pulse height distribution on electrode *n* equal to *the sum* of the distributions shown in figure 15(*b*). This is because electrode *n* receives electron pulses not only from particles arriving directly above it but also from particles arriving above adjacent electrodes.

Figures 16 and 17 show experimental confirmation of (i) and (ii). A narrow ion beam was used in the experiments of figure 16. The counts measured in a fixed time interval are plotted as a function of PHDL (note that when the PHDL is varied, all detectors vary simultaneously). Differentiation of this data gives the distribution of voltage pulse heights on the electrodes. It is this distribution of pulse heights which determines the FWHM of a measured peak and hence determines the resolving power

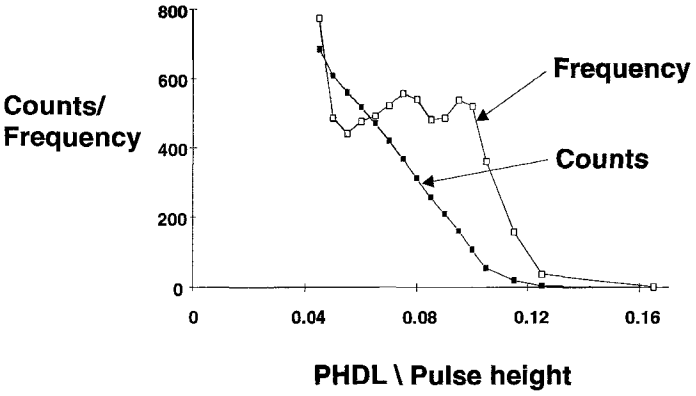

Figure 17. Counts measured as a function of PHDL for a broad beam covering the whole array. This is differentiated to show the pulse height distribution (maximum normalized to 800). The MCP voltage was 2 kV and the MCP/array separation was between 4·5 and 10 microns.

of the array module. By reducing the PHDL more of the pulse height distribution will lie above the discrimination level and more counts will be detected on peripheral electrodes resulting in wider peaks. The pulse height distributions themselves (and hence the resolving power of the detector array) depend on the MCP gain, the distance of separation between the MCP output and the detector electrodes, capacitative cross coupling between detector electrodes, etc.

Figure 17 shows the pulse height distribution obtained on any electrode when the array module is uniformly illuminated. As the PHDL is reduced there is a monotonic increase of the observed count rate because the pulse height distribution includes low amplitude pulses from remote events. As the PHDL is lowered a plot of count rate versus PHDL will not show the plateau characteristic of a stable operating region.

5.3. *Dynamic range*

The dynamic range is fully specified by giving the maximum and minimum count rate capabilities of the system. The total system comprises three components—the MCP, the array and the data acquisition system. We consider each component separately and take a *single* detector of the array. It should be remembered that the maximum total count rate capability of the array is m times that of a single detector where m is the number of detectors.

MCP

Approximately 1000 MCP channels service a single detector, each channel having a recovery time of about 0·01 s giving a maximum count rate of about 10^5 Hz. The MCP generates on average 1 'dark' count per cm^2 per second. As 1 cm^2 of a MCP with a channel pitch of 15 microns contains approximately 5×10^5 channels a single channel gives on average 1 dark count in 5×10^5 seconds. Hence 1000 channels give on average 1 dark count in 5×10^2 seconds, i.e. a dark count rate of about 2×10^{-3} Hz.

Array

The maximum count rate allowed by the charge pulse sensor circuitry is about 5×10^6 Hz. In the absence of a MCP supply voltage we have been unable to detect noise on any of 192 detectors over a period of several minutes. Therefore noise

Downloaded At: 17:09 21 January 2011

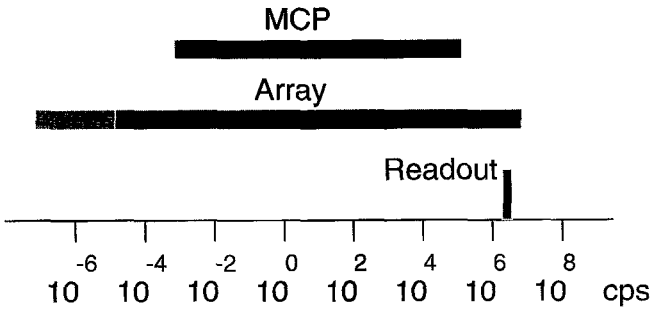

Figure 18. The dynamic range of the Aberystwyth detector array system. The count rate range is indicated. The lower limit of the array is less than 10^{-5} counts per second.

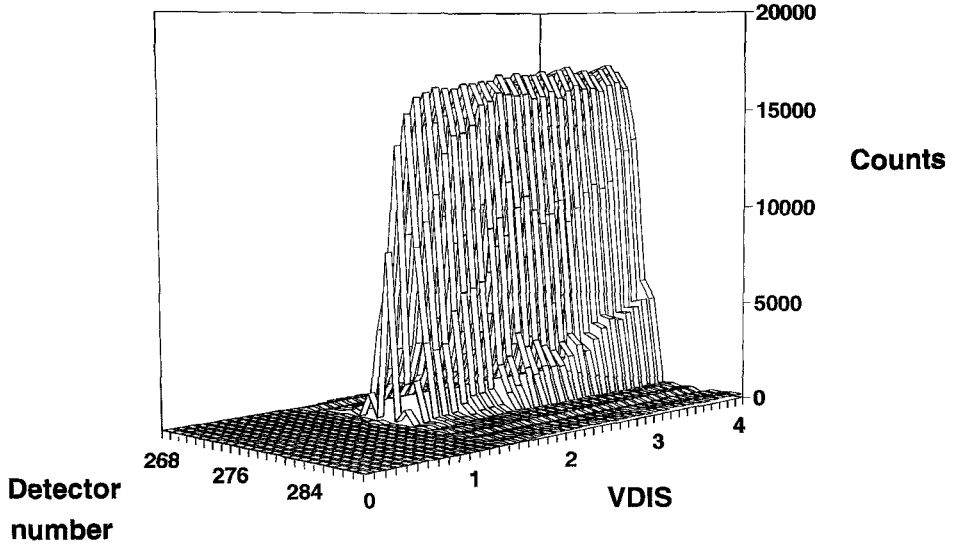

Figure 19. Measured ion peak shown as a function of VDIS at MCP voltage, 2·2 kV. An increasing VDIS corresponds to a decreasing PHDL.

generated by the array per detector is much less than the MCP dark counts and is $< 10^{-5}$ Hz.

Data acquisition system

Consider the array of 192 detectors each with its own 8 bit counter operating in mode 2 (§5.1). The data acquisition system must read and store the array data. A custom interface could read the array at a rate limited by the array itself (currently 3 MHz). However, the array is normally connected directly to a PC and data can be acquired at typically $\leqslant 1$ MHz i.e. 192 counters are read in $\geqslant 192 \times 10^{-6}$ s. The maximum count rate would therefore be 254 counts (i.e. a full 8 bit counter) in 192×10^{-6} s or $\sim 1{\cdot}3 \times$ MHz. If the array were 5 cm long containing 2000 detectors the maximum count rate per detector set by the readout rate would be about $1{\cdot}3 \times 10^5$ Hz. When operating in modes 1 or 3 the maximum count rate is not limited by the data acquisition system but by the array module. There is no minimum rate set by the data acquisition system. The dynamic range of the present array module is therefore dominated by the MCP performance as shown in figure 18.

Downloaded At: 17:09 21 January 2011

5.3.1. *Resolving power*

A high resolution spectrometer must focus particles to give narrow well-focused peaks at the detector. The slit width of a single slit detector can be simply reduced to match the peak width (§3.3). In the case of a discrete electrode detector array there is no slit and a given detector is influenced by the high gain MCP output pulses of remote events. This gives a broadening of the measured peaks and hence a loss of resolving power. We define the resolving power of the array module as the FWHM of a measured peak where the particle beam FWHM is less than one detector pitch (25 microns in the present case) wide.

Figure 19 shows the N_2^+ peak measured as a function of the detector discrimination level at a MCP supply voltage of 2·2 kV [40]. VDIS is a voltage input to the array which controls the PHDL [40]. It can be seen that as the PHDL is decreased (VDIS increased) the peak widens and the peak maximum reaches a plateau.

From such data over a range of MCP voltages the FWHM of the peak can be found as a function of MCP voltage and PHDL and plotted as a contour diagram. Figure 20(*a*) shows the results for a separation between the MCP and the array of about 25 microns. Figure 20(*b*) differs from figure 20(*a*) in that the separation between the MCP and the array is reduced to about 4·5 microns.

The contour diagrams summarize concisely the resolving power of the array module. They can best be described in terms of the idealised contour diagram of figure 21 which shows the contour diagram divided into three regions.

Region 1—No signal is detected at low MCP voltages and high PHDL.
Region 2—As the FWHM increases the peak maximum also increases. Events are first detected when the PHDL is reduced below the upper limit of the pulse height distribution (figure 15). At this point the minimum FWHM of 1 is observed. As the PHDL is reduced (for a given MCP voltage) the peak maximum and width increase as more of the pulse height distribution lies above the PHDL. It should be noted that the variation of peak height is not shown on the contour diagrams.
Region 3—As the FWHM increases, the peak maximum remains constant. This is the region of stable operation and is observable only if the particle beam is narrow (§5.2). Within this region the pulse height distribution on the electrode at the peak centre lies completely above the PHDL.

The FWHM = 4 contour was found experimentally to be the approximate location of the boundary between regions 2 and 3 in figures 20(*a*) and (*b*). This has been interpreted as indicating that the electron pulse at the MCP exit covers about four electrodes [36].

A contour diagram summarises the factors influencing the width of a measured peak. These factors include:

MCP voltage—a larger MCP voltage gives a higher gain and this leads to pulse widening due to space charge repulsion. In addition to this the effect of capacitatively induced pulses on adjacent electrodes increases.
PHDL—a lower PHDL enables detection of lower amplitude pulses on electrodes remote from the centre of electron pulses.
MCP/array separation—larger separation enables greater electron pulse spreading.
MCP/array bias voltage—an attractive voltage on the array helps to confine electron pulses and reduce spreading.
Capacitative cross coupling—capacitatively induced pulses on detector electrodes adjacent to central electrodes can cause peak broadening.

Downloaded At: 17:09 21 January 2011

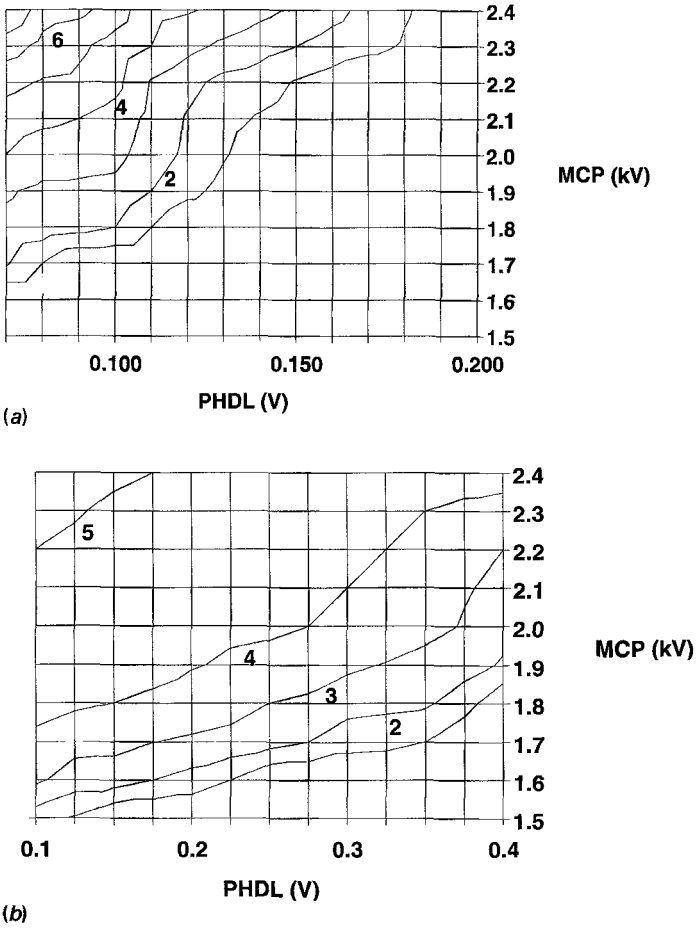

Figure 20. FWHM of measured peaks as a function of detector discrimination level and the MCP modal gain. Contours show the location of constant FWHM in units of detector pitch (25 microns). A two stack MCP was used with the plates in intimate contact. The MCP voltage was applied between the front and rear of the stack with the contacting faces finding their own level. (*a*) MCP/array separation between 25 and 50 microns. (*b*) MCP/array separation between 4·5 and 10 microns. The same MCP stack but different arrays were used for experiments (*a*) and (*b*).

All of these factors have been included in a simulation of the array module using Mathcad [41]. The space charge spreading of the electron pulse was calculated using the method of Vibrans [42]. Acceptable agreement was obtained between experimental and simulated contour diagrams. The simulator is currently being used to help in the design of higher resolving power arrays.

5.3.2. *Uniformity*

It is essential that when an ion beam is measured at different positions on an array the same peak profile is seen. This may not be the case for several reasons:

- as the width of the detector electrodes, the MCP channel diameters and the particle beam width are similar, the registration of the beam with the MCP channels and the electrodes influences the measured peak shape. This can be

Downloaded At: 17:09 21 January 2011

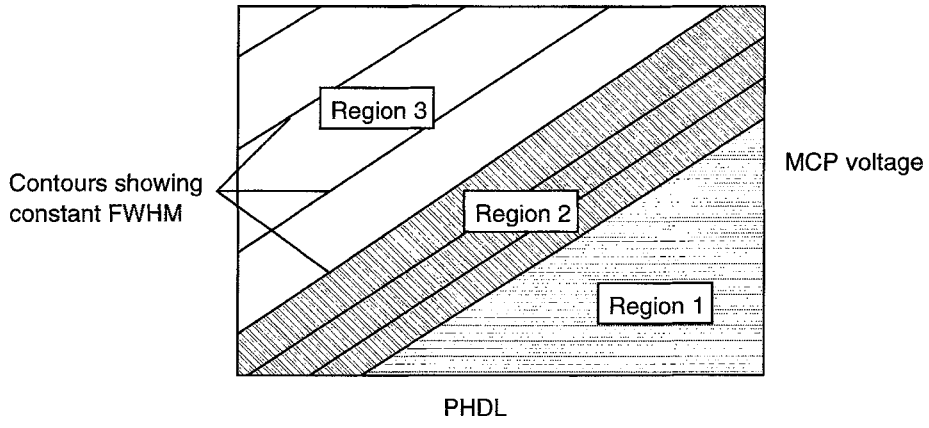

Figure 21. Idealized contour diagram for a narrow particle beam. In region 1 no signal is detected. In region 2 the peak maximum increases as the FWHM increases. In region 3 the peak maximum remains constant as the FWHM increases.

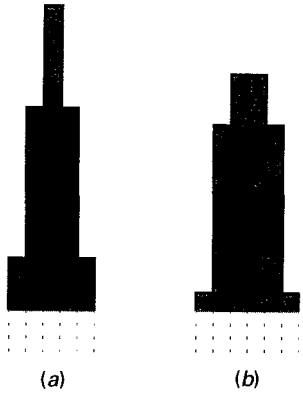

Figure 22. Schematic of the tops of peaks measured with the same ion beam but shifted across the array to give (*a*) the peak centred above a detector electrode, (*b*) the peak centred between two electrodes.

clearly seen when a peak is moved gradually across an array. With the ion beam centred above an electrode the pulse height distribution lies at the highest values on this electrode giving a peak maximum as shown in figure 22(*a*). When the beam is centred between electrodes two equal distributions on adjacent electrodes lie at somewhat lower values giving a peak maximum as in figure 22(*b*). As the PHDL is reduced the measured peaks widen and the maxima converge to the same value hence much reducing this effect.

- charge sensor design. The electrical design and the layout of the charge sensor is of central importance but is outside the scope of this paper.
- MCP quality and accuracy of mounting. As can be seen from figure 20 the MCP/array separation has a large effect on performance and hence it must be ensured that the MCP is equidistant from the detector electrodes over the whole array.
- positioning in the spectrometer focal plane. If the front face of the MCP is not in the focal plane of the spectrometer then a peak profile will differ across the array.

Downloaded At: 17:09 21 January 2011

A solution to the problem of non-uniformity is to sample each part of a spectrum with each detector by moving the spectrum across the array and accumulating the data. While this may give an acceptable result it is desirable to optimize the uniformity as far as is possible.

These issues are currently being pursued at Aberystwyth. Software corrections to residual non-uniformity are also under study.

6. Conclusions

Single slit detectors sacrifice collection efficiency in order to excel in other respects. For the highest resolution work the single slit is currently the best option.

Single event position sensitive detectors currently offer low cost, a good resolving power and a high collection efficiency but only at low particle flux.

Electro-optical arrays incorporating a CCD represent an attractive combination of resolving power, dynamic range and collection efficiency. However, these devices are larger and more complex than integrated discrete electrode arrays and as analogue devices do not have the advantage of counting statistics. In addition they must be cooled for low noise operation.

Discrete electrode detector arrays integrated on silicon offer a unique combination of low noise, power, size and complexity with high resolving power and dynamic range. The array developed at Aberystwyth was produced using 3 micron CMOS technology. Sub-micron CMOS processes are now available which, in conjunction with wafer scale integration design techniques, offer the prospect of much longer, higher resolving power arrays. Development costs of such arrays may be high but on completion of the design the production cost will be relatively low. These devices are poised to benefit from the rapid advances in silicon technology.

Downloaded At: 17:09 21 January 2011

Acknowledgments

This paper is dedicated to my PhD supervisor Professor Michael J. Henchman on his 60th birthday with happy memories of the active, stimulating research environment, and the opportunities which arose as a result of a year (1967–68) spent completing my PhD work in the USA.

The initial development of the Aberystwyth array was carried out under a LINK Industrial Measurements Systems programme with the support of the SERC, DTI, VG Analytical Ltd., ICI (Wilton), the Microelectronics Groups at the Rutherford–Appleton Laboratory and Hughes Microelectronics Europa Ltd. The further support of the Higher Education Funding Council for Wales, the British Mass Spectrometry Society, the Joy Welch Educational Trust and the University of Wales Aberystwyth Research Fund is gratefully acknowledged. The author is indebted to Mr D. P.Langstaff for his work on the array design and experimentation and to many others who have contributed to the project.

References

[1] McClintock, W. E., Barth, C. A., Steele, R. E., Lawrence, G. M., and Timothy, J. G., 1982, *Appl. Optics*, **21**, 3071.

[2] Timothy, J. G., and Bybee, R. L., 1975, *Appl. Optics*, **14**, 1632.

[3] Kellogg, E., Henry, P., Murray, S., and Van Speybroeck, L., 1976, *Rev. Sci. Instrum.*, **47**, 282.

[4] Padmore, T. S., Roberts, K. M., Padmore, H. A., and Thornton, G., 1988, *Nucl. Instrum. Methods in Phys. Res.*, **A270**, 582.

[5] HICKS, P. J., DAVIEL, S., WALLBANK, B., and COMER, J., 1980, *J. Phys.* E, **13**, 713.
[6] RICHTER, L. J., and HO, W., 1986, *Rev. Sci. Instrum.*, **57**, 1469.
[7] ADAMS, N. G., and SMITH, D., 1974, *J. Phys.* E, **8**, 759.
[8] ABERTH, W., 1981, *Int. J. Mass Spectrom. Ion Processes*, **37**, 379.
[9] LIPTAK, M., SANDIE, W. G., SHELLEY, E. G., and SIMPSON, D. A., 1984, *IEEE Trans. Nucl. Sci.*, **NS-31**, 780.
[10] GURNEY, B. A., HO, W., RICHTER, L. J., and VILLARUBIA, J. S., 1988, *Rev. Sci. Instrum.*, **59**, 22.
[11] COTRELL, J. S., and EVANS, S., 1987, *Rapid Commun. Mass Spectrom.*, **1**, 1.
[12] JORDAN, P., 1994, *Phys. World*, **7**, 40.
[13] WELLS, A., and POUNDS, K., 1993, *Phys. World*, **6**, 32.
[14] KENNERLEY, S., WIGHT, H., LITTLE, D., KIMBER, M., and MOORE, C., 1993, in Proceedings of the 20th Annual British Mass Spectrometry Society Meeting, p. 34.
[15] MOAK, C. D., DATZ, S., GARCIA, F., SANTIBANEZ, G., and CARLSON, T. A., 1975, *J. Electron Spectros. Related Phen.*, **6**, 151.
[16] FIRMANI, C., RUIZ, E., CARLSON, C. W., LAMPTON, M., and PARESCE, F., 1982, *Rev. Sci. Instrum.*, **53**, 570.
[17] LAMPTON, M., and CARLSON, C. W., 1979, *Rev. Sci. Instrum.*, **50**, 1093.
[18] Hamamatsu Photonics (Hamamatsu City, 435 Japan), Position Sensitive Detector type S1352 technical data sheet (1993).
[19] GOTT, R., PARKES, W., and POUNDS, K. A., 1970, *IEEE Trans. Nucl. Sci.*, **17**, 367.
[20] VAN HOOF, H. A., and VAN DER WIEL, M. J., 1980, *J. Phys.* E, **13**, 409.
[21] TIMOTHY, J. G., and BYBEE, R. L., 1981, *SPIE*, **265**, 93.
[22] MARTIN, C., JELINSKY, P., LAMPTON, M., MALINA, F., and ANGER, H. O., 1981, *Rev. Sci. Instrum.*, **52**, 1067.
[23] BOETTGER, H. G., GIFFIN, C. E., and NORRIS, D. D., 1979, ACS Symposium Series 102, *Multichannel Image Detectors*, edited by Y. Talmi (American Chemical Society) p. 291.
[24] HATFIELD, J. V., YORK, T. A., COMER, J., and HICKS, P. J., 1989, *IEEE J. Solid State Circuits*, **24**, 704.
[25] LANGSTAFF, D. P., LAWTON, M. W., MCGINNITY, T. M., FORBES, D. M., and BIRKINSHAW, K., 1994, *Meas. Sci. and Technol.*, **5**, 389.
[26] HATFIELD, J. V., BURKE, S. A., COMER, J., CURRELL, F., GOLDFINCH, J., YORK, T. A., and HICKS, P. J., 1992, *Rev. Sci. Instrum.*, **63**, 235.
[27] TIMOTHY, J. G., 1981, *Rev. Sci. Instrum.*, **52**, 1131.
[28] WIZA, J. L., 1979, *Nucl. Instrum. Methods*, **162**, 587.
[29] Galileo Electro-Optics Corporation, (Galileo Park, P.O. Box 550, Sturbridge, MA 01566, USA), Technical Information sheet PB3-6/94-5K.
[30] BIRKINSHAW, K., and LANGSTAFF, D. P., 1994, *Int. J. Mass Spectrom. Ion Processes*, **132**, 193.
[31] FRASER, G. W., 1984, *Nucl. Instrum. Methods* **221**, 115.
[32] LOTY, C., 1971, *Acta Electronica* **14**, 107.
[33] ANACKER, D. C., and ERSKINE, J. L., 1991, *Rev. Sci. Instrum.*, **62**, 1246.
[34] SCHMIDT, K. C., and HENDEE, C. F., 1966, *IEEE Trans. Nucl. Sci.*, **NS–13**, 100.
[35] Hamamatsu, (Hamamatsu City, 435 Japan), Technical information sheet, 'MCP assembly', (1991).
[36] LANGSTAFF, D. P., and BIRKINSHAW, K., 1995, *Rapid Commun. Mass Spectrom.*, **9**, 703.
[37] BIRKINSHAW, K., International patent publication number WO91/00612 (submitted 1989).
[38] BIRKINSHAW, K., MCGINNITY, T. M., LANGSTAFF, D. P., LAWTON, M. W., and FORBES, D. M., 1991, *Sensors Technology, Systems and Applications* (Adam-Hilger) pp. 421–426.
[39] BIRKINSHAW, K., 1992, *The Analyst*, **117**, 1099.
[40] BIRKINSHAW, K., and LANGSTAFF, D. P., 1994, *Int. J. Mass Spectrom. Ion Processes*, **136**, 71.
[41] NARAYAN, D. J., LANGSTAFF, D. P., and BIRKINSHAW, K. 1995, *Int. J. Mass Spectrom. Ion Processes* (in press).
[42] VIBRANS, G. E., 1963, Computation of the spreading of an electron beam under acceleration and space charge repulsion, Technical Report No. 308, Lincoln Laboratory, Massachusetts Institute of Technology.

Downloaded At: 17:09 21 January 2011